A Fuzzy-Statistical Contour Model for MRI Segmentation and Target Tracking

Wael Abd-Almageed[a], Aly El-Osery[b], and Christopher E. Smith[c]

[a]Computer Vision Laboratory
Institute for Advanced Computer Studies
University of Maryland at College Park
wamageed@umiacs.umd.edu

[b]Electrical Engineering Department
New Mexico Institute of Mining and Technology
elosery@ee.nmt.edu

[c]Robotics, Artificial Intelligence and Vision Laboratory
Department of Electrical and Computer Engineering
University of New Mexico
chsmith@eece.unm.edu

ABSTRACT

In this paper, a new formulation for the parametric active contour model is presented. The new formulation is based on statistical pattern recognition theory. A hybrid of kernel density estimation and fuzzy logic is used to show that active contours can be thought of as a pattern recognition problem. The proposed approach is used in two different application domains, with different performance requirements, to demonstrate its effectiveness. First, the proposed approach is used for a magnetic resonance image segmentation problem to demonstrate the segmentation accuracy. Second, the contour is used in a target tracking experiment to show its tracking capabilities.

Keywords: Active Contours, Snakes, Kernel Density Estimation, Parzen Window, MRI Segmentation, Target Tracking

1. INTRODUCTION

Active contours were first introduced in 1987 by Kass et al.[1] Active contours, more commonly known as snakes, are elastic splines that iteratively deform to object boundaries in the given image. Snakes have been used in different applications such as medical image segmentation[2] and robot vision.[3] One of the main advantages of active contours is that they give a piece-wise linear description of the shape of the object at the time of convergence, without extra processing. Other stated advantages include tolerance to image noise.

One of the major drawbacks of active contours is the strong dependency on finding strong image gradients to drive the contour. This drawback, in deed, significantly limits the use of the active contours. In this paper, we propose a new fuzzy-statistical approach that overcomes this drawback. Via the proposed approach, we show that active contours, in fact, can be thought of in terms of the classical pattern recognition framework. We apply the proposed approach to the problems of magnetic resonance image (MRI) segmentation and target tracking. The two problems pose different performance requirements.

This paper is organized as follows. Section (2) presents a brief background on active contours and discusses the previously mentioned drawback in more details. In Section (3), the proposed approach is presented. The results of the two experiments are demonstrated in Section (4). Finally, the paper is concluded with direction to future research in Section (5).

For further information please contact the first author.

2. BACKGROUND

Snakes are energy-minimizing splines. The contour is continuously moving in order to minimize its energy. At the minimum-energy state, the contour is said to *converge*. The set of forces that control the deformation of the contour are internal forces, image force, and external forces. Tension force and curvature force are the two internal forces responsible for maintaining the cohesiveness and smoothness of the contour. Tension is responsible for achieving equal point spacing for the contour. Curvature, on the other hand, is responsible for maintaining a certain degree of smoothness for the contour. The image forces drive the snake toward certain image features such as edges, lines or corners. External forces are user-defined forces that may be applied to enforce certain characteristics of the contour. The original energy functional, given by Kass et al.,[1] of the contour is given by

$$E = \int_0^1 E_{\text{Snake}}(S(u))du, \tag{1}$$

where u represents the snake points and $S(u)$ represents the snake. The snake's energy, E_{Snake}, at a certain point, u, is the weighted sum of the internal energy, the image energy or potential (edges, corners, or dark spots on the image) and external energy (e.g., employing user-selected points as attractors). The external energy term could be used to reshape the contour, biasing it toward some local shape. Equation (2) describes the total energy of the snake.

$$E = \int_0^1 (E_{\text{Internal}}(S(u)) + E_{\text{External}}(S(u)) + E_{\text{Image}}(S(u)))du \tag{2}$$

In its most common form, image energy is estimated as the result of edge detection. For example, the image energy can be computed as[1]

$$E_{\text{Image}} = -(G_\sigma \otimes \bigtriangledown^2 I)^2, \tag{3}$$

where the Laplacian, $\bigtriangledown^2$, of the image I is convolved with a Gaussian kernel, G_σ. The result is squared to account for positive and negative edges, and the negative of this magnitude is used in order to attract the contour to a local minima. The image energy term is calculated from the image edges in the neighborhood around each control point of the snake. The energy is minimized when a control point is located on the steepest part of the gradient. Most snakes in use today are based upon Kass et al. snakes and they retain the use of edge detection as a measure of image gradient.

One of the first problems associated with the traditional formulations of Kass et al.[1] is that in the absence of image gradient these models tended to collapse. Therefore, a strong gradient field is preferred to drive the snake. On the other hand, in strong gradient fields the initial placement of the snake has to be carefully chosen, so that the snake does not collapse to a local minimum away from the object. In fact, a segment of the snake must cross the gradient associated with the region of interest. A question now arises; If we have the strong edges needed to drive the snake, why do we have to use snakes? In other words, why do we not use a simpler edge linking technique, to segment the object of interest?

To overcome these limitations, balloon snakes were developed by Cohen[4] where they added a new internal pressure term to force the model to expand. Unfortunately, the new pressure term introduces new problems with the model. For instance, the initial placement of the snake had to be within the target (a constraint that still remains in many models). Also, in weak gradient fields, the balloon snakes tend to explode rather than collapse. The proposed solution by Ronfard[5] was a dynamic pressure model. Ronfard's method incorporated a term that, by computing the similarity of pixel values around the snake control points, created a force that would push the points toward region boundaries. Scale spaces were used to capture region boundaries that lie outside the local neighborhood.

Ivins and Porrill[6] paralleled this line of research by proposing several forms of dynamic pressure models. These models overcome the need to change scales by having a region well defined not just locally but across the entire image. The pressure models are based upon low order statistics and utilize a seed region of the image to identify positive versus negative pressure regions. In other words, image regions that are statistically similar to the seed region yield positive pressure while image regions that are some number of standard deviations away from the seed yield negative pressure. When a portion of the contour is in a positive region, it will expand the contour. When a portion of the contour is in a negative region, it will contract. It follows that the minimum energy of the contour lies on the pressure boundary between the positive and negative pressure regions. This work can be viewed as the application of statistical segmentation to the image.

The pressure force used by Ivins and Porrill[6] is as follows. A seed region is selected from within the target. The mean μ and standard deviation σ of the intensity for the seed region are computed. The image force is then given by:

$$\vec{F}(S(u)) = \left(1 - \frac{|I(S(u)) - \mu|}{k\sigma}\right)\left(\frac{\partial S(u)}{\partial u}\right)^{\perp}, \tag{4}$$

where S is the curve and k is a user specified parameter, that signifies the Bayesian decision boundary. The $\perp$ indicates that the image force is perpendicularly applied to the tangent of the contour. This model is a linear pressure model where the image force increases linearly away from a zero when the image intensity is k standard deviations to either side of the mean.

The pressure model of Equation (4) represented the object of interest using low order statistics. Also, the model did not account for the background characteristics. Finally, the free parameter k had to be manually tuned.

In[7] and[8] Abd-Almageed et al. introduced a statistically optimal method for estimating the free parameter k. Furthermore, they introduced a generic pressure model the accounts for complex foreground and background characteristics.

3. APPROACH

As we stated earlier, the main objective is to show that the contour evolution is in fact a feature classification problem. Therefore, any appropriate feature classifier can be used to drive the active contour and to obtain satisfactory results. A generic pressure force that is to be used to drive the contour can be of the form

$$\vec{F}(S(u)) = \mathcal{P}(p(\mathbf{x}|\mathcal{O}), p(\mathbf{x}|\mathcal{B}))\left(\frac{\partial S(u)}{\partial u}\right)^{\perp}, \tag{5}$$

where the function $\mathcal{P}(.,.)$ is a generic pressure function parameterized by the statistical properties of the object and the background, $p(\mathbf{x}|\mathcal{O})$, is the density function of the object features and $p(\mathbf{x}|\mathcal{B}))$ is the density function of the background features. The density functions $p(\mathbf{x}|\mathcal{O})$ and $p(\mathbf{x}|\mathcal{B})$ are estimated using the kernel density estimator introduced by Parzen[9] and given by Equation (6)

$$p(x) = \frac{1}{h}\frac{1}{N}\sum_{i=1}^{N}\Phi\left(\frac{x_i - x}{h}\right), \tag{6}$$

where Φ is called the kernel function and is given by

$$\Phi(\mathbf{x}) = \frac{1}{\sqrt{2\pi}}\exp\left(-\frac{1}{2}\mathbf{x}^T\mathbf{x}\right). \tag{7}$$

Our goal now is to design a fuzzy system, representing the feature classifier, that approximates $\mathcal{P}$ without having to determine a closed-form for the relationship between the object and background statistical characteristics $p(\mathbf{x}|\mathcal{O})$ and $p(\mathbf{x}|\mathcal{B})$. To achieve this objective, a fuzzy rule-based system is designed as shown in Figure (1). The membership functions are the same for both the object probability input and the background probability input and are shown in Figure (2). Because of the similar nature of the two inputs, the membership functions for both inputs are similar. The membership functions of the fuzzy system output, i.e. the pressure to be applied to the contour point, are shown in Figure (2). Table (1) shows the linguistic rules used to map the input space into the output space. The fuzzy rules here represent the opinion of an expert.

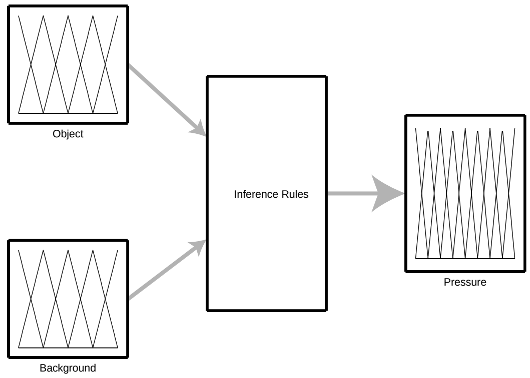

Figure 1. Fuzzy System

Background and Object Probability Membership Functions.

Pressure Membership Functions.

Figure 2. Membership Functions for the Fuzzy-Statistical Contour.

Table 1: Fuzzy Rules used to Drive the Contour

IF *Obj. Prob.* is LOW and *Bckgrnd. Prob.* is LOW, THEN *Pressure* is 0
IF *Obj. Prob.* is LOW and *Bckgrnd. Prob.* is LOW-MED., THEN *Pressure* is -1
IF *Obj. Prob.* is LOW and *Bckgrnd. Prob.* is MED., THEN *Pressure* is -2
IF *Obj. Prob.* is LOW and *Bckgrnd. Prob.* is MED.-HI., THEN *Pressure* is -3
IF *Obj. Prob.* is LOW and *Bckgrnd. Prob.* is HI., THEN *Pressure* is -4
IF *Obj. Prob.* is LOW-MED. and *Bckgrnd. Prob.* is LOW, THEN *Pressure* is 1
IF *Obj. Prob.* is LOW-MED. and *Bckgrnd. Prob.* is LOW-MED., THEN *Pressure* is 0
IF *Obj. Prob.* is LOW-MED. and *Bckgrnd. Prob.* is MED., THEN *Pressure* is -1
IF *Obj. Prob.* is LOW-MED. and *Bckgrnd. Prob.* is MED.-HI., THEN *Pressure* is -2
IF *Obj. Prob.* is LOW-MED. and *Bckgrnd. Prob.* is HI., THEN *Pressure* is -3
IF *Obj. Prob.* is MED. and *Bckgrnd. Prob.* is LOW, THEN *Pressure* is 2
IF *Obj. Prob.* is MED. and *Bckgrnd. Prob.* is LOW-MED., THEN *Pressure* is 1
IF *Obj. Prob.* is MED. and *Bckgrnd. Prob.* is MED., THEN *Pressure* is 0
IF *Obj. Prob.* is MED. and *Bckgrnd. Prob.* is MED.-HI., THEN *Pressure* is -1
IF *Obj. Prob.* is MED. and *Bckgrnd. Prob.* is HI., THEN *Pressure* is -2
IF *Obj. Prob.* is MED-HI. and *Bckgrnd. Prob.* is LOW, THEN *Pressure* is 3
IF *Obj. Prob.* is MED-HI. and *Bckgrnd. Prob.* is LOW-MED., THEN *Pressure* is 2
IF *Obj. Prob.* is MED-HI. and *Bckgrnd. Prob.* is MED., THEN *Pressure* is 1
IF *Obj. Prob.* is MED-HI. and *Bckgrnd. Prob.* is MED.-HI., THEN *Pressure* is 0
IF *Obj. Prob.* is MED-HI. and *Bckgrnd. Prob.* is HI., THEN *Pressure* is -1
IF *Obj. Prob.* is HI. and *Bckgrnd. Prob.* is LOW, THEN *Pressure* is 4
IF *Obj. Prob.* is HI. and *Bckgrnd. Prob.* is LOW-MED., THEN *Pressure* is 3
IF *Obj. Prob.* is HI. and *Bckgrnd. Prob.* is MED., THEN *Pressure* is 2

IF *Obj. Prob.* is HI. and *Bckgrnd. Prob.* is MED.-HI., THEN *Pressure* is 1
IF *Obj. Prob.* is HI. and *Bckgrnd. Prob.* is HI., THEN *Pressure* is 0

4. EXPERIMENTAL RESULTS

To visualize the relationship between the inputs and the output of the fuzzy system we simulated the response of the fuzzy system for different values of object and background probabilities. Figure (3) shows the results of the simulation. The obtained surface is highly nonlinear. It is clear from the figure that, because of the nonlinearities, it is difficult to obtain a closed-form solution for the relationship between the foreground and background features.

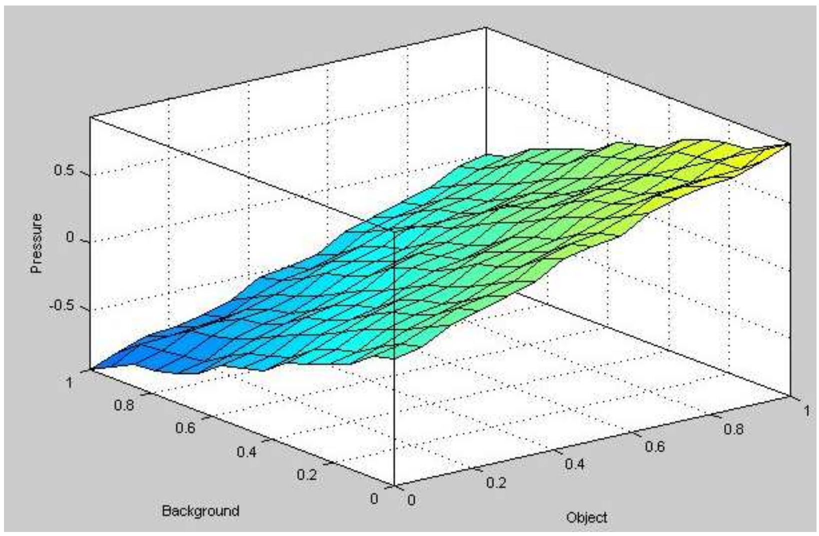

Figure 3. Input-Output Relationship of the Fuzzy Pressure System

4.1. Magnetic Resonance Image Segmentation

The active contour, driven by the model of Equation (5), was applied to a set of magnetic resonance images. The experiments are conducted on gray-scale MR images to demonstrate the effectiveness of the proposed approach on data with low dimensionality.

The snake-based segmentation of the cerebellum is shown in Figure (4). Figure (5) demonstrates the performance of the proposed snake model by segmenting the Lateral Ventricle area in an axial view. In Figure (6) and Figure (7), the proposed contour model was applied to segment the Lateral Ventricle from a Coronal and Sagittal views, respectively.

In Figure (8) the proposed contour model was applied to two snakes to segment some brain abnormalities. The two snakes are used to segment the inner and the outer contours of the abnormality. Finally, we show the performance of the proposed contour model by segmenting a brain lobe as shown in Figure (9). The snakes performs with high degree of segmentation accuracy, regardless of the large area of the lobe and its complexity.

4.2. Target Tracking

The segmentation of magnetic resonance images demonstrates the performance of the proposed contour model when a high level of accuracy is needed. The contour model of Equation (5) was then applied to a target tracking application to demonstrate the real-time tracking capabilities of the proposed approach. In tracking applications, the main objective is to accurately track the target area, with an acceptable level of segmentation accuracy. In other words, we need to maintain a reasonable estimate of the location of the target area with less emphasis with respect to its shape.

Figure 4. Snake segmentation of the Cerebellum area. The Medulla area is included in the segmentation as a result of the imperfect MR scanning.

Figure 5. Snake segmentation of the Lateral Ventricle area from an Axial view.

The colors of the target area (white shirt and black pants) are specifically selected such that they span the entire gray scale, to maximize the overlap between the density function of the target and the density function of the background. Also, the target area was specifically selected such that it does not include the face and hand areas of the target to demonstrate the effectiveness of the proposed contour model.

Figures (10) and (11) illustrate the tracking results for the video sequence. For this sequence, we used a 30-point active contour. A tracking rate of 20 frame/second was achieved, on a 1GHz P-III machine, running Microsoft Windows 2000. The tracking code was written in C and is not fully optimized.

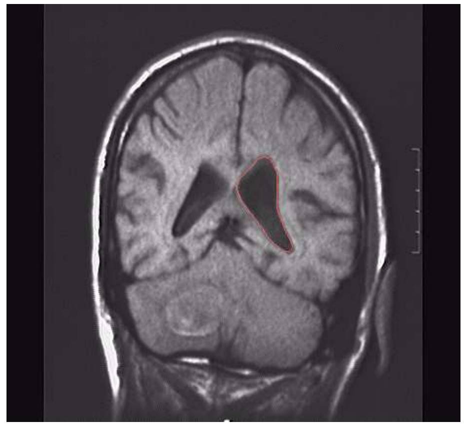

Figure 6. Snake segmentation of the Lateral Ventricle area from a Coronal view

Figure 7. Snake segmentation of the Lateral Ventricle area from a Sagittal view

Figure 8. Snake segmentation of Brain Abnormality

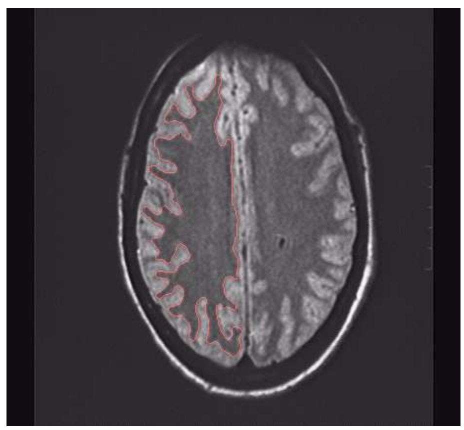

Figure 9. Snake segmentation of Brain Lobe

Frame No. 0.

Frame No. 10.

Frame No. 20.

Frame No. 30.

Frame No. 40.

Frame No. 50.

Frame No. 60.

Frame No. 70.

Frame No. 80.

Frame No. 90.

Frame No. 100.

Frame No. 110.

Frame No. 120.

Frame No. 130.

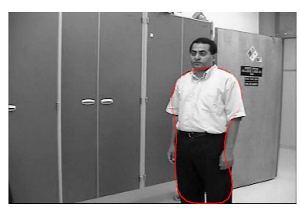

Frame No. 140.

Figure 10. Fuzzy Tracking with 30-Control Point Snake.

  

Frame No. 150. Frame No. 160. Frame No. 170.

  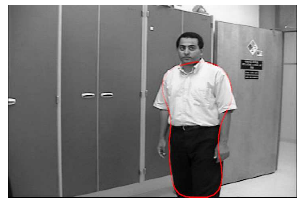

Frame No. 180. Frame No. 190. Frame No. 200.

  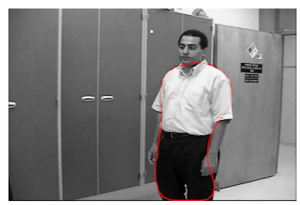

Frame No. 210. Frame No. 220. Frame No. 230.

  

Frame No. 240. Frame No. 250. Frame No. 260.

  

Frame No. 270. Frame No. 280. Frame No. 290.

Figure 11. Fuzzy Tracking with 30-Control Point Snake.

5. CONCLUSIONS

In this paper, a new formulation for the active contours was presented. Fuzzy sets were used to compute the image forces required to drive the contour toward salient image features. The designed fuzzy system acts as a feature classifier based on the estimated statistical characteristics of both the target and background features.

The proposed approach was used in two different application domains with different performance requirements. In MRI segmentation applications the main emphasis is on the accuracy of the segmentation with less emphasis on the speed of convergence of the contour. In target tracking applications, on the other hand, the most important requirement is to maintain a good estimate of the target location, with a reasonable segmentation accuracy. High degree of segmentation accuracy was demonstrated when the proposed approach was applied to a set of MR imagery. In the mean time, the proposed contour model demonstrated near-real-time performance when applied to a target tracking problem.

The results obtained in this paper suggest that any appropriate feature classifier can be used to drive the contour toward the required image features. In X-ray segmentation applications, the gray level cannot be used as a distinguishing feature. It is customary to use higher-dimensional features in such applications. Therefore, it becomes necessary to use feature classifiers that are appropriate in these situations. We plan to use support vector machines (SVM) classifier to drive the contour for segmenting X-ray imagery.

REFERENCES

1. M. Kass, A. Witkin, and D. Terzopoulos, “Snakes: Active Contour Models,” in *First International Conference on Computer Vision*, 1987.
2. S. Fenster, C.-B. G. Kuo, and J. Kender, “Nonparametric Training of Snakes to Find Indistinct Boundaries,” in *Workshop on Mathematical Methods in Biomedical Image Analysis*, IEEE, December 2001.
3. D. Perrin, O. Masoud, C. Smith, and N. Papanikolopoulos, “Using Fast Statistical Dynamic Contours for Grasping Occluding Contours,” in *Proc. 8th Mediterranean Conference on Control and Automation*, 2000.
4. L. Cohen, “On Active Contour Models and Balloons,” *Computer Vision, Graphics and Image Processing: Image Understanding* **53**, pp. 211–218, 1991.
5. R. Ronfard, “Region-based Strategies for Active Contour Models,” *International Journal on Computer Vision* **13**, p. 229, 1994.
6. J. Ivins and J. Porrill, “Active Region Models for Segmenting Medical Images,” in *Proceedings of the IEEE Internation Conference on Image Processing*, 1994.
7. W. Abd-Almageed and C. E. Smith, “Mixture Models for Dynamic Statistical Pressure Snakes,” in *IEEE International Conference on Pattern Recognition, Quebec City, Canada*, 2002.
8. W. Abd-Almageed, C. E. Smith, and S. Ramadan, “Kernel Snakes: Non-Parametric Active Contour Models,” in *IEEE International Conference on Systems, Man and Cybernetics*, 2003.
9. E. Parzen, “On the Estimation of a Probability Density Function and the Mode,” *Ann. Math. Statistics* **33**, pp. 1065–1076, 1962.